Heliyon 10 (2024) e34120

Contents lists available at ScienceDirect

Heliyon

journal homepage: www.cell.com/heliyon

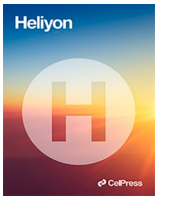

Research article

NMDA receptor remodeling and nNOS activation in mice after unilateral striatal injury with 6-OHDA

Michele Barboza de Carvalho [a,1], Bruna Teixeira-Silva [a,1], Suelen Adriani Marques [b,c], Andrea Alice Silva [d], Marcelo Cossenza [e], Adriana da Cunha Faria-Melibeu [f], Claudio Alberto Serfaty [g], Paula Campello-Costa [a,*]

[a] *Laboratory of Neuroplasticity, Postgraduate Program in Neurosciences, Biology Institute, Fluminense Federal University, Niteroi, RJ, Brazil*
[b] *Laboratory of Neural Regeneration and Function, Department of Neurobiology, Federal Fluminense University, Niteroi, RJ, Brazil*
[c] *Postgraduate School in Pathological Anatomy, Federal University of the State of Rio de Janeiro, Brazil*
[d] *Multiuser Laboratory for Research Support in Nephrology and Medical Sciences (LAMAP), Graduate Program in Pathology, Faculty of Medicine, Universidade Federal Fluminense, Niterói, 24033-900, Rio de Janeiro, Brazil*
[e] *Laboratory of Molecular Pharmacology, Physiology and Pharmacology Department, Biomedical Institute, Postgraduate Program in Neurosciences, Biology Institute, Fluminense Federal University, Niteroi, RJ, Brazil*
[f] *Laboratory of Neurobiology of Development, Postgraduate Program in Neurosciences, Biology Institute, Fluminense Federal University, Niteroi, RJ, Brazil*
[g] *Laboratory of Neural Plasticity, Postgraduate Program in Neurosciences, Biology Institute, Fluminense Federal University, Niteroi, RJ, Brazil*

ARTICLE INFO

Keywords:
Parkinson's disease
6-OHDA
PSD-95
NMDA receptor
Nitric oxide

ABSTRACT

Parkinson's disease (PD) is a progressive neurodegenerative disorder characterized by selective dopaminergic loss. Non dopaminergic neurotransmitters such as glutamate are also involved in PD progression. NMDA receptor/postsynaptic density protein 95 (PSD-95)/neuronal nitric oxide synthase (nNOS) activation is involved in neuronal excitability in PD. Here, we are focusing on the evaluating these post-synaptic protein levels in the 6-OHDA model of PD. Adult male C57BL/6 mice subjected to unilateral striatal injury with 6-OHDA were assessed at 1-, 2-, or 4-weeks post-lesion. Animals were subjected to an apomorphine-induced rotation test followed by the analysis of protein content, synaptic structure, and NOx production. All biochemical analysis was performed comparing the control *versus* lesioned sides of the same animal. 6-OHDA mice exhibited contralateral rotation activity, difficulties in coordinating movements, and changes in Iba-1 and glial fibrillary acidic protein (GFAP) expression during the whole period. At one week of survival, the mice showed a shift in NMDA composition, favoring the GluN2A subunit and increased PSD95 and nNOS expression and NOx formation. After two-weeks, a decrease in the total number of synapses was observed in the lesioned side. However, the number of excitatory synapses was increased with a higher content of GluN1 subunit and PSD95. After four weeks, NMDA receptor subunits restored to control levels. Interestingly, NOx formation in the serum increased. This study reveals, for the first time, the temporal course of behavioral deficits and glutamatergic synaptic plasticity through NMDAr subunit shift. Together, these data demonstrate that dopamine depletion leads to a fine adaptive response over time, which can be used for further studies of therapeutic management adjustments with the progression of PD.

* Corresponding author. Programa de Neurociências, Instituto de Biologia, Universidade Federal Fluminense, Niterói, CEP, 24001-970, RJ, Brazil.
E-mail addresses: paulacampello@id.uff.br, pcampello.lopes@gmail.com (P. Campello-Costa).
[1] Carvalho, MB and Teixeira-Silva, B contribute equally as co-authors.

https://doi.org/10.1016/j.heliyon.2024.e34120
Received 11 January 2024; Received in revised form 6 June 2024; Accepted 3 July 2024
Available online 4 July 2024

Abbreviation section

6-OHDA – 6-hydroxydopamine
CNS - Central Nervous System
DAPI - 4′,6-Diamidino-2-fenilindol, 2-(4-Amidinofenil)-6-indolecarbamidina
GFAP - Glial Fibrillary Acidic Protein
GluN1, GluN2A and GluN2B - Subunits of NMDA receptor
Iba-1 - Ionized calcium-binding adaptor molecule 1
MPTP - 1-methyl- 4-phenyl-1, 2, 3, 6-tetrahydropyridine
NMDAr - N-methyl-D-aspartate receptors
nNOS - Neuronal Nitric Oxide Synthase
NO - Nitric Oxide
NOx – Nitric oxide metabolites (nitrate and nitrite)
PD - Parkinson's disease (PD)
PSD-95 - Postsynaptic density protein 95
RIPA - radioimmunoprecipitation assay (RIPA) buffer

1. Introduction

Parkinson's Disease (PD) is a progressive neurodegenerative disorder characterized by motor [1] and non-motor [2,3] symptoms as a consequence of the selective loss of dopaminergic neurons at the substantia nigra pars compacta [4,5]. Several studies demonstrated intense crosstalk between dopaminergic receptors and NMDARs (N-methyl-D-aspartate receptors) via direct physical association to reciprocally regulate receptor surface expression, channel properties, and downstream intracellular signaling cascades [6–8].

NMDA receptors are tetrameric complexes extensively expressed in the CNS [9–11]. The rat and human striatum are enriched in GluN1, GluN2A, and GluN2B subunits [12,13], and depending on the composition of the subunits that form the NMDA channel, different functional properties are observed [10]. Also, the NMDAR function seems to be partially dependent on the postsynaptic density protein of 95 KDa (PSD-95) which interacts with and activates neuronal nitric oxide synthase (nNOS). NMDAR hypofunction can result in cognitive deficits, whereas overstimulation causes excitotoxicity and subsequent neurodegeneration, including in PD [14–17].

Although NMDAR signaling pathway has been used as a possible therapeutic strategy for different CNS disorders [17,18], additional studies are necessary to determine the better strategy to modulate NMDA function in different stages of Parkinson's disease.

Herein, we investigate the time course of synaptic plasticity, focusing on evaluating the protein levels of NMDARs subunits, PSD-95, and nitric oxide in a 6-OHDA mouse model of PD.

2. Material and methods

2.1. Animals

A total of 59 animals (n = 59) were obtained from a laboratory animals center (Fluminense Federal University, Brazil) and maintained under controlled light and environmental conditions (12 h light/12 dark cycle at a constant temperature of 22 °C) with free access to food and water were used in this study.

All animal use procedures were in strict accordance with The National Institutes of Health (NIH, USA) Guide for the Care and Use of Laboratory Animals and were approved by the local animal care committee under protocol number 244. Studies were designed to minimize the number of animals used and their pain and suffering.

2.2. Surgery procedures

Adult male mice C57BL/6 (3 months) were anesthetized with a mixture of ketamine and xylazine (i.p. 100 mg/kg and 25 mg/kg, respectively) and placed in a stereotaxic apparatus. Animals underwent unilateral striatal lesions with an intracranial injection of 6-hydroxydopamine neurotoxin (2 μL of a 0.9 % saline solution containing 2.96 mg/mL 6-OHDA and 0.02 % ascorbic acid-Sigma-Aldrich) at a rate of 0.5 μL/5 min. The injection was performed using the following stereotaxic coordinates from Bregma: AP 0.5 mm; ML 2.0 mm, DV- 3.0 mm from the brain surface [19]. The micropipette was withdrawn after a further 5 min to minimize backflow of the 6-OHDA solution. Mice received postoperative care until they were awake and then returned to their home cages. The mortality rate after 6-OHDA injection was zero.

2.3. Rotation test

1-, 2-, or 4-weeks post-surgery, animals were subjected to motor behavior test in an open field arena (50 cm × 60 cm, Insight) after apomorphine i.p. injection (5 mg/kg diluted in 0,09 % saline solution; Sigma). Apomorphine-induced contralateral rotations were

recorded for 20 min with a digital camera [20]. Afterward, animals were used for biochemical and immunohistochemical experiments.

2.4. Immunofluorescence

After different post-lesion survival times, mice were deeply anesthetized with an overdose of 5 % isoflurane and perfused through the left cardiac ventricle with 0.9 % NaCl solution followed by 4 % paraformaldehyde in phosphate buffer saline (PBS) pH 7.4. The brains were removed and left for post-fixation in the same fixative solution at 4 °C for 30 min. The brains were cryoprotected in 15 % followed by 30 % sucrose solution in PBS at 4 °C, overnight, frozen and cut in 10 μm slices at coronal orientations. The slices were washed and incubated overnight at 4 °C with polyclonal anti-GFAP from rabbit (1:300, Cell Signaling #3670), polyclonal anti-Iba-1 from rabbit (1:100, Wako # 019–19741), polyclonal anti-PSD-95 antibody from rabbit (1:250, Cell signaling #3450), anti-nNOS from rabbit (1:200, Cell Signaling mAb4231). All antibodies were diluted in 2 % BSA (bovine serum albumin, Sigma). After washing with PBS, tissue sections were incubated with Alexa Fluor 488 secondary antibody diluted 1: 200 in 0.4 % PBS and 2 % BSA (goat anti-rabbit-IgG; green fluorescence; Invitrogen #A-11008) at room temperature for 90 min. Afterward, sections were washed, counter-staining with DAPI (Sigma) and coverslips mounted using fluorescence medium (4 % n-propyl gallate in phosphate buffer/80 % glycerol) (Merck). Control sections were processed in the absence of primary antibodies. Sections were analyzed under a deconvolution microscope (Leica, Germany).

2.5. Western blot analysis

For the biochemical assays, mice were deeply anesthetized as above, decapitated and striatal tissue was dissected and homogenized in ice-cold with radioimmunoprecipitation assay (RIPA) buffer (Thermo Scientific - 25 mM Tris-HCl pH 7.6, 150 mM NaCl, 1 % NP-40, 1 % sodium deoxycholate, 0.1 % SDS) + EDTA + proteinase inhibitors (Thermo Scientific). Protein concentration was measured by the method of Bradford [21]. The analysis of proteins contents was carried out in total membranes of striatal samples (40 μg protein/lane) which were separated by SDS/PAGE (8 or 10 % concentrating gel) and electro-transferred to PDVF membrane (polyvinylidene difluoride membranes, Amersham Biosciences, Piscataway, NJ, USA). After blocking for 2 h at room temperature with 5 % defatted milk in Tris-buffered saline, pH 7.6 containing 0.1 % Tween 20 (TBS-T), the membranes were incubated overnight at 4^{o}C with specific antibodies: polyclonal anti-GFAP from rabbit (1:2500, Cell Signaling #3670), polyclonal anti-Iba-1 from rabbit (1:100, Wako # 019–19741), polyclonal anti-rabbit PSD-95 (1:250, Cell signaling #3450), anti-rabbit nNOS (1:200, Cell Signaling #mAb4231), anti-goat GluN1 (1:1000, Santa Cruz #SC1467), anti-mouse GluN2A (1:500, Millipore #MAB5216) and anti-goat GluN2B (1:500, Santa Cruz Biotechnology #SC1469). After washing with TBS-T (3 × 10 min), the membranes were incubated with a specific secondary antibody (1:5000 dilution, Invitrogen) in TBS-T for 1 h at room temperature. After six washing periods of 5 min in TBS-T, the membranes were revealed using Luminata chemiluminescent (Amersham Bioscience) with a Chemi Express system (Loccus). Either anti-extracellular signal-regulated kinase (ERK - 1:1000, Santa Cruz Biotechnology #sc-514302) or anti-alpha tubulin (1:50000, Cell Signaling #3873) antibodies were used as a loading control. The densitometry analysis was performed in Scion Image Software, Version 4.03 (Scion Corporation, MD, USA). At least three independent runs were performed with samples originating from different animals. All gels revealed for the same protein were quantified on the same day by the same researcher. The Scion Image program assigns arbitrary values based on the density of the individual bands. Results obtained in each sample of lesioned striatum (LES) were normalized as a percentage of corresponding inner control (non-lesioned side - CTL)

2.6. Griess reaction

The striatum from 6-OHDA lesioned animals was homogenized using 200 μl of RIPA buffer + EDTA + protease inhibitors (Thermo Scientific). Supernatants were prepared with a clear, protein-free filtrate by centrifugation at 10.000×*g* for 10 min at 4 °C after treatment with $ZnSO_4$ 15 g/L. To prepare serum samples, after euthanizing the animals to dissect the brain tissue, blood samples were quickly collected by cardiac puncture, centrifuged at 10000 g, and stored at −80^{o}C until use [22,23].

Determination of nitric oxide levels (NOx) was performed by a colorimetric assay after incubation of supernatant with vanadium III and Griess reagent (2 % in sulfanilamide HCl 5 % and 0.1 % nafitiletilenodiamida in water) at a 96-well microtiter plate for 30 min at room temperature. The standard curve was performed using sodium nitrite and nitrate standard of 0.8–100 μM. Total nitrite was determined at 540 nm using the spectrophotometer Vesamax (Molecular Device, USA). NOx represents the total concentration of nitrite plus nitrate [22,23].

2.7. Electron microscopy analysis

For ultrastructural analysis of synapses, samples from the caudate and putamen nuclei of 2 weeks post-surgery 6-OHDA mice and controls were fixed with 2.5 % glutaraldehyde diluted in 0.1 M phosphate buffer and post-fixed by immersion in 1 % osmium tetroxide in cacodylate buffer with 0.8 % potassium ferrocyanide for 6 h at room temperature. The samples were washed three times with 0.1 M phosphate buffer (pH 7.4), dehydrated with a graded acetone series, embedded in resin, and polymerized for 48 h at 60 °C. Ultrathin sections (70 nm) were collected in copper grids (300 mesh) and analyzed under the transmission electron microscope (JEM 1001, Jeol) with a digitalizing image system (Gatan). A total of fifty images at 30.000× magnification were acquired per animal/experimental condition (n = 3 animals - control and lesioned side) and performed the quantitative synaptic analysis under double-blinded manner. Synaptic profiles were identified by presynaptic vesicles and postsynaptic membrane specialization (with or without evident synaptic

cleft). All synapses in the micrographs were counted. Image J free software (NIH) was used to quantify the total number of synapses in the neuropil and to evaluate the relationship between excitatory and inhibitory synapses. A total area of 380 μm^2 per animal (n = 3 per group) was counted, and we described it as the total number of synapses per area [24].

2.8. Statistics

Graphs were plotted using Prism 7.0 software and the statistical analysis was performed using one-way ANOVA with Tukey post-test for multiple comparisons or unpaired Student's t-test and differences were considered significant when $p < 0.05$. The data are shown as the mean and standard error of the mean (SEM) for all analyses.

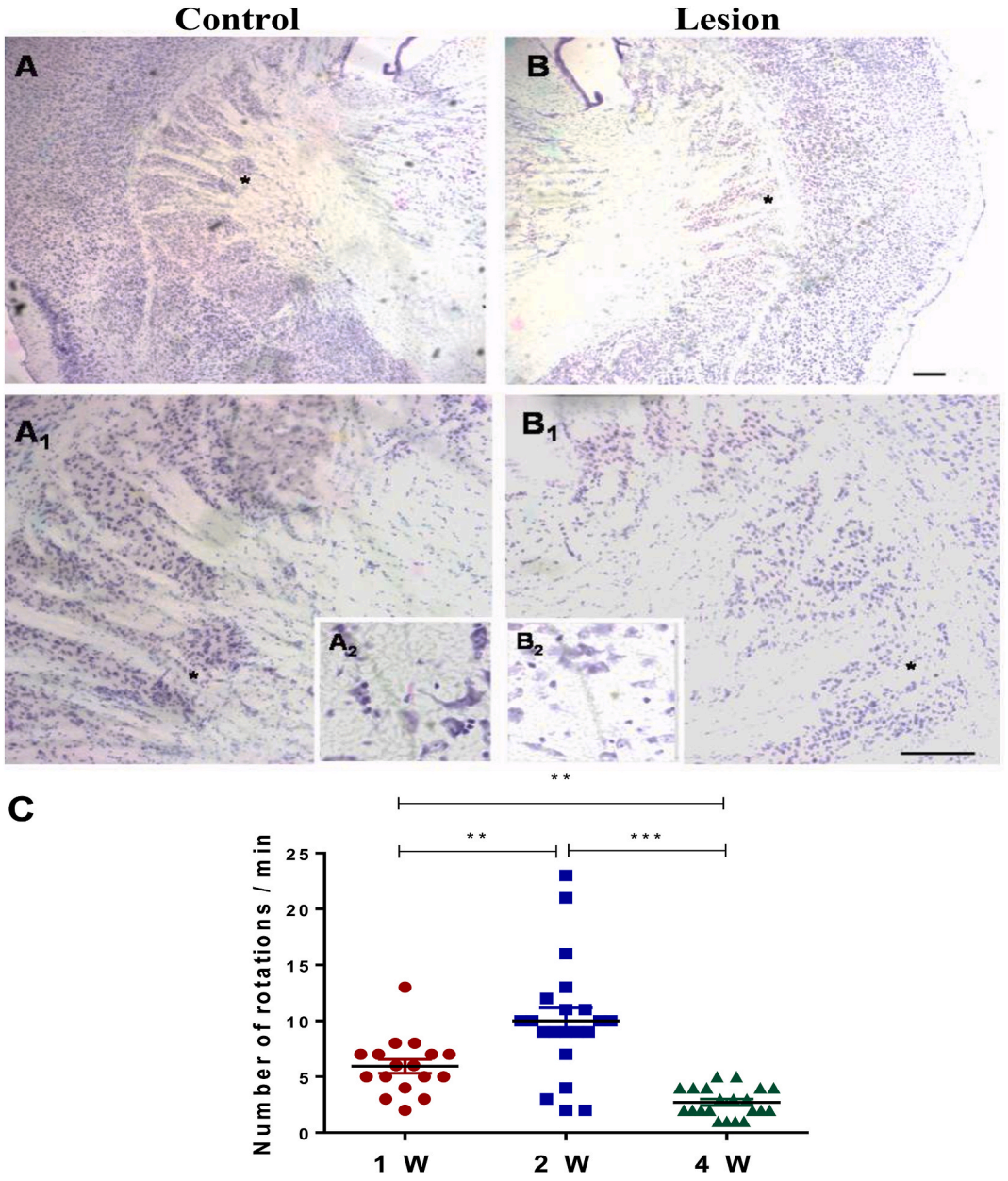

Fig. 1. Cellular and behavior analyses in 6-OHDA injected animals. (A–B) Representative sections of the Nissl staining of the striatum in two-weeks after lesion in 6-OHDA mice (n = 3 animals). Note that the injured side presented a reduction in the cell labeling compared to control one. (A, B) 20X, (A′ B′) 40X, (A′′e B″) 100X (C) Time-course of apomorphine-induced rotation after 6-OHDA injection. **p < 0,05 related to 1W, ***p < 0.001 between 2W and 4 W groups. n = 17 animals at 1w; n = 21 animals for the 2w and 4w group.

3. Results

3.1. Time course of behavioral and glial response after 6-OHDA lesion

The intrastriatal injection of 6-OHDA has been used to study different aspects of PD [25,26]. Fig. 1 shows that the striatum on the lesioned side with 6-OHDA (Fig. 1B,B_1,B_2) displays a less organized structure with a reduction in Nissl staining compared to the non-lesioned control side (Fig. 1A,A_1,A_2). Also, all animals presented, after one week of survival, an apomorphine-induced contralateral rotation (5941 ± 0,6152 rotations/min) confirming that 6-OHDA mice presented cellular and behavior characteristics previously described [26]. Interestingly, we observed that the mice exhibited, two weeks after lesion, a more pronounced rotation profile (10 ± 1289 rotation/min), while the four-weeks survival group showed the lowest rate of rotation (2714 ± 0,2857 rotation/min) (Fig. 1C). Glial cells are critical for proper brain function, and changes in their state can contribute to different neurological pathologies, such as Parkinson's disease [27,28]. To analyze possible alterations in glial cells in 6-OHDA mice, GFAP and Iba-1 protein,

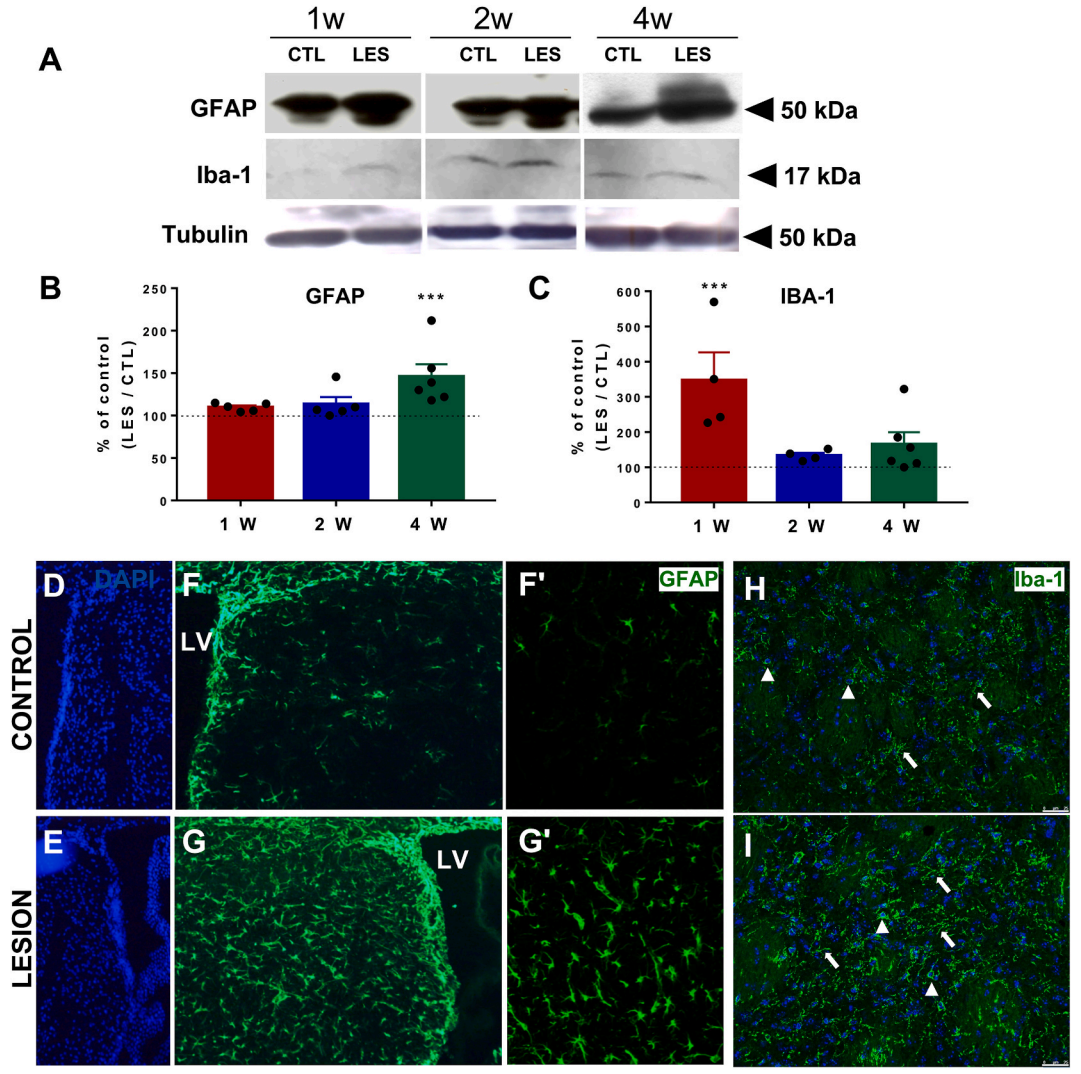

Fig. 2. Glial markers in the striatum of mice after 6-OHDA injection. (A) Representative Western blot for GFAP (top) and Iba-1 (bottom) in the control (CTL) and lesioned (LES) side of striatum of 6-OHDA mice after 1, 2 or 4 weeks of survival. Densitometry analysis of GFAP (B) and Iba-1 (C) contents in the lesioned striatum (lesion) relative to the control matched-side for each time-point. (GFAP - n = 5 animals for 1w and 2w; n = 6 animals for the 4w group; Iba-1 - n = 4 animals for 1w and 2w; n = 6 animals for the 4w group). Data represents the mean ± S.E.M. ***p < 0,01 (ANOVA followed by Tukey's test). DAPI staining in the control (D) and lesioned (E) striatum. Immunofluorescence for GFAP (green) in control (F and F′) and lesioned (G and G′) striatum after four-week survival post-lesion. Iba-1 immunodetection (green) merged with DAPI in control (H) and lesioned (I) striatum of 1-week post-lesion animals. Note an increased staining intensity for both GFAP and Iba-1 in the lesioned striatum. The arrows indicate the cell processes, and the arrowheads indicate the cell bodies. N = 3 animals/group. 400 x. Scale bar: 25 μm. (See Supplemental Fig. S2a).

which are astrocytic and microglial markers, respectively, were evaluated. Fig. 2 shows an increase in GFAP level on the lesioned side, particularly in the four weeks of survival (Fig. 2A, B, 2G, 2G′) compared to control side (Fig. 2F,F′). On the other hand, Iba-1 protein was increased at one week after the lesion (Fig. 2A, C and 2I) compared to the control side (Figure H). DAPI staining was used to label cell nuclei (Fig. 2D and E). Collectively these data showed that there is a specific time course for the behavioral effects and glial response induced by 6-OHDA.

3.2. *Synaptic alterations and differential response of glutamatergic receptors in 6-OHDA mice*

Synaptic density was evaluated ultra-structurally two weeks after the striatal lesion. Synaptic profiles were identified by the presence of the postsynaptic density and presynaptic vesicles (Fig. 3A–D). We found that the total synapse number was decreased by 15 % in lesioned striatum, compared with the control side (Fig. 3E). The analyses of the synaptic profile revealed a significant increase in asymmetric (excitatory) synapses and a tendency to decrease the symmetric (inhibitory) synapses in lesioned striatum (Fig. 3E).

An increase in glutamate signaling has been reported in PD patients [29,30]. Since we found an increase in excitatory synapses in our model, we decided to investigate the profile of NMDA receptor subunits. One week after the lesion, we observed a slight decrease in GluN1 subunit, an increase in GluN2A subunit and a decrease in GluN2B subunit of NMDAR (Fig. 4A,B,C,D). On the other hand, at two

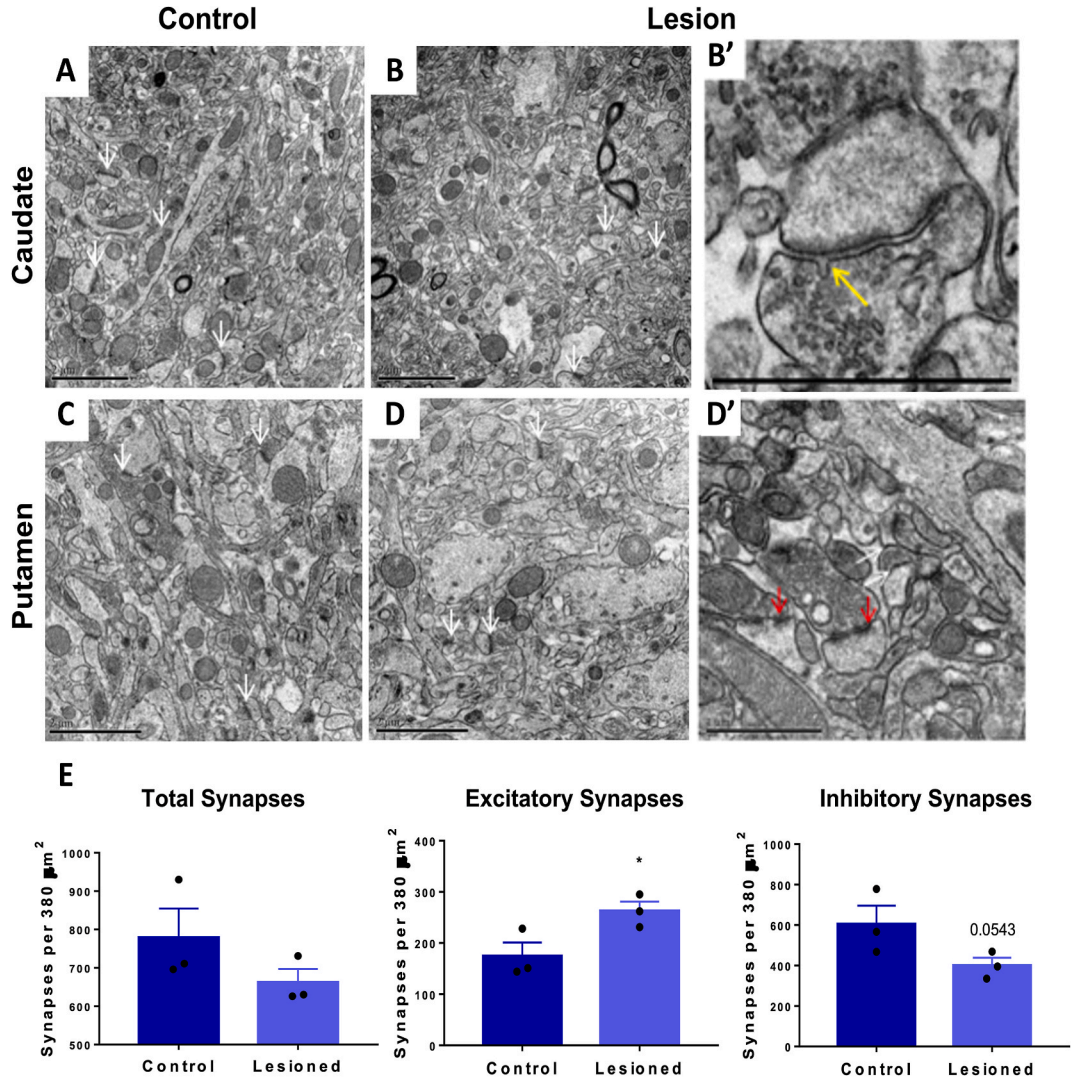

Fig. 3. Ultrastructural analyses of synapses in animals 2 weeks after 6-OHDA injection. Striatal cytoarchitecture of control (A, C) and lesioned (B, D) sides. White arrows indicate synapses in the neuropil. (B′, D′) Representative images of lesioned striatum synapses. The yellow arrow shows a vesicle fusing into the presynaptic terminal membrane. The red arrows point to the synaptic cleft. (E) Quantification of the total number of synapses and the number of excitatory and inhibitory synapses. Data represents the mean ± S.E.M. *p < 0,05. (Unpaired T-test). N = 3 animals. Scale bar: 2 μm.

weeks of survival, only GluN1 was increased in the lesioned striatum (Fig. 4A and B). Four weeks after injury, the level of GluN1 was restored while GluN2B decreased compared to the non-lesioned side (Fig. 4A,B,D). Next, we assessed the PSD-95 content and observed an increase in this protein over time, being more evident two weeks after lesion (Fig. 4A–E).

3.3. The modulation of nitric oxide in 6-OHDA mice

The nitric oxide (NO) participates in important functions such as synaptic plasticity, neuromodulation, and neurotransmission. In neurons, the NO interacts with the NMDA receptors through the association between PSD-95 and nNOS [31,32]. Also, NO takes part in regulation of several aspects of PD such as excitotoxicity, inflammation, oxidative stress, among others [33]. For this reason, we decided to analyze the nNOS content and NOx products in 6-OHDA mice. Fig. 5 shows a transient increase in both nNOS protein (Fig. 5A) and NOx production (Fig. 5C) only one week after the lesion. Immunofluorescence analysis indicates a similar cellular distribution of nNOS in both control and lesioned sides, characterized by immunolabeling in the cell body and neuronal processes (Fig. 5B). Interestingly the NOx analysis in the serum revealed an increase only after four-weeks survival post-lesion (Fig. 5D). The interaction of PSD-95 with nNOS to increase NOx production is already well described [33,34]. So, we carried out a double labeling for these proteins in the context of PD. Fig. 6 shows that there is a strong colocalization of PSD-95 and nNOS both in the control (Fig. 6A–C) and in the injured (Fig. 6B–D) side of the striatum, suggesting a coupling between these proteins in the animal model of 6-OHDA.

4. Discussion

Parkinson's Disease is a neurodegenerative disorder that currently affects over 8 million people worldwide and is characterized by the presence of motor and non-motor symptoms (https://www.who.int/news-room/fact-sheets/detail/parkinson-disease). It's one of the leading causes of disability nowadays and its prevalence is projected to double in the next twenty years [35]. Therefore, studying novel mechanisms behind the pathophysiology of PD is essential. The intracerebral injection of 6-hydroxydopamine (6-OHDA) has been studied in different species such as mice, rat, cats, dogs, and monkeys [36–38], representing a useful model to study PD pathogenesis that mimic the late-stage of PD patients [39,40]. Likewise humans, it has been shown that there are differences between the sexes, as male rats are more susceptible to the effects of 6-OHDA than females [41,42]. Herein, we used the 6-OHDA unilateral striatal injection in male mice which is a gold standard since it is well tolerate by the animal, highly reproductible and shows classical features of PD [38,43]. Besides, unilateral injection allows to use the non-lesioned hemisphere as an internal control to study the cellular and

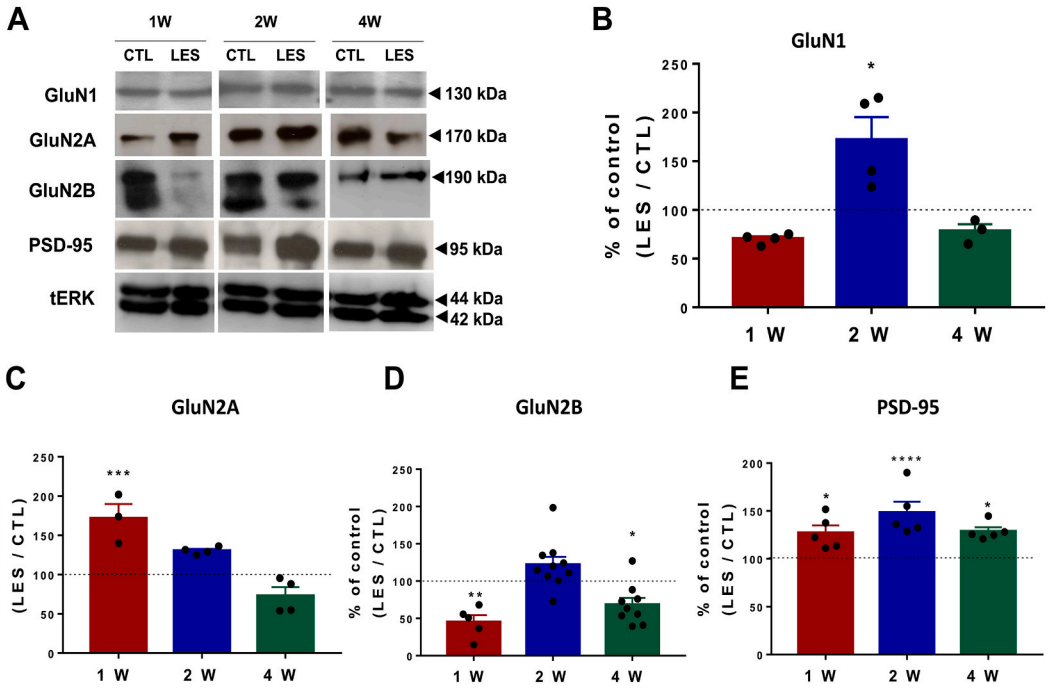

Fig. 4. Glutamatergic receptors and PSD-95 content in the striatum of mice model of PD. (A) Representative Western blot for GluN1, GluN2A, GluN2B and PSD-95 of control (CTL) and lesioned (LES) sides of striatum of 6-OHDA mice after 1, 2 or 4 weeks of survival. tERK was used as a loading control. Densitometric analysis of GluN1(B), GluN2A (C), GluN2B (D) and PSD-95 (E) contents in the lesioned striatum relative to the control matched-side for each time-point (GluN1 - n = 4 animals for 1w and 2w; n = 3 animals for the 4w group; GluN2A - n = 3 mice for 1w; n = 4 mice for the 2w and 4w groups; GluN2B - n = 5 mice for 1w; n = 10 mice for 2w; n = 9 mice for the 4w group; PSD-95 - n = 5 animals for each survival time). Data represents the mean ± S.E.M. *p < 0,05, ***p < 0,001, ****p< 0,0001 (ANOVA followed by Tukey's test). (See Supplemental Fig. S4a).

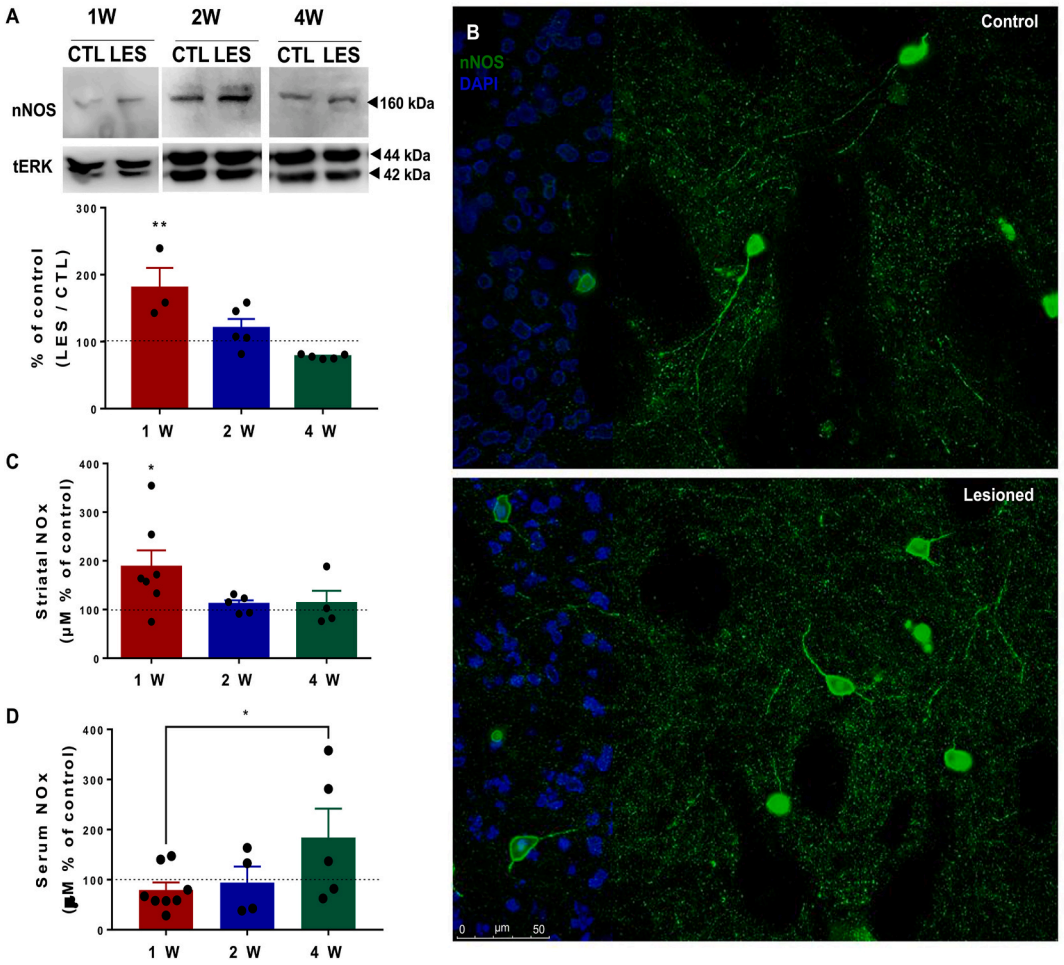

Fig. 5. nNOS content and NOx production in 6-OHDA mice. (A) Representative Western blot for nNOS in the striatum of 6-OHDA mice after 1, 2 or 4 weeks of survival (top) and densitometric analysis (bottom) of nNOS contents in the lesioned (LES) striatum compared to the control (CTL) side for each time-point (n = 3 animals for 1w; n = 5 animals for 2w and 4w groups). (B) Immunoreactivity for nNOS (green) in the control (top) and lesioned (bottom) striatum of 6-OHDA mice, one week after lesion. DAPI stainning (blue) was used for cell staining (n = 3 animals). 40x. Scale bar: 50 µm. (C) NOx products in the lesioned striatum after different survival times post-lesion relative to the control matched-side for each time-point. n = 7 animals for 1w; n = 5 animals for 2w; n = 4 animals for the 4w group. (D) NOx products in the serum after different survival times post-lesion relative to the control matched-side for each time-point. n = 8 animals for 1w; n = 4 animals for 2w; n = 5 animals for the 4w group. Data represents the mean ± S.E.M. *p < 0,05, ***p < 0,01 (ANOVA followed by Tukey's test). (See Supplemental Fig. S5a).

molecular mechanisms underlying the neurodegeneration and leads to a classic rotational behavior which can be useful to test new therapeutic strategies. There is a minimum dopaminergic neurons loss at the substantia nigra pars compacta and striatum, one week after 6-OHDA injection and it reaches a peak within 2–3 weeks [25,40]. In addition, changes in other neurotransmitter systems such as glutamate have already been identified [12,17,44,45]. Therefore, we decided to evaluate the time course of synaptic changes, focusing mainly on the NMDA receptor, PSD-95, and NO contents in a 6-OHDA model. We chose to evaluate the animals at 1-, 2- or 4-weeks post-injury to investigate possible glutamatergic plastic adjustments before, during and after the highest peak of dopaminergic degeneration described in the model.

Firstly, to test the success of the injection, we subjected 6-OHDA mice to an apomorphine injection according to previous works [20]. We observed that the animals presented an apomorphine-induced contralateral rotation after one-week post-lesion, being more pronounced after two weeks (Fig. 1C). At four weeks, post-injury we observed the lowest number of rotations, which could reflect an improvement in behavior over time. However, animals still presented motor deficits previously described at all times of survival such as akinesia, bradykinesia, and jaw movements, suggesting a severe motor impairment. Additionally, the Nissl analysis of the striatum demonstrated a disorganized structure with less staining in the lesioned side compared to matched-control sides (Fig. 1A and B) confirming the presence of motor symptoms of PD during this period. Besides, increasing evidence has demonstrated that both microglial activation and a prolonged astrocyte dysfunctions affect the pathogenesis and progression of PD [46–51]. Analysis of GFAP and Iba-1, astroglial and microglial markers, revealed a rapid increase in Iba-1 content one week after injury and a later increase in GFAP at four weeks post-injury (Fig. 2). This is in accordance with previous data showing a more rapid increase in microglia than

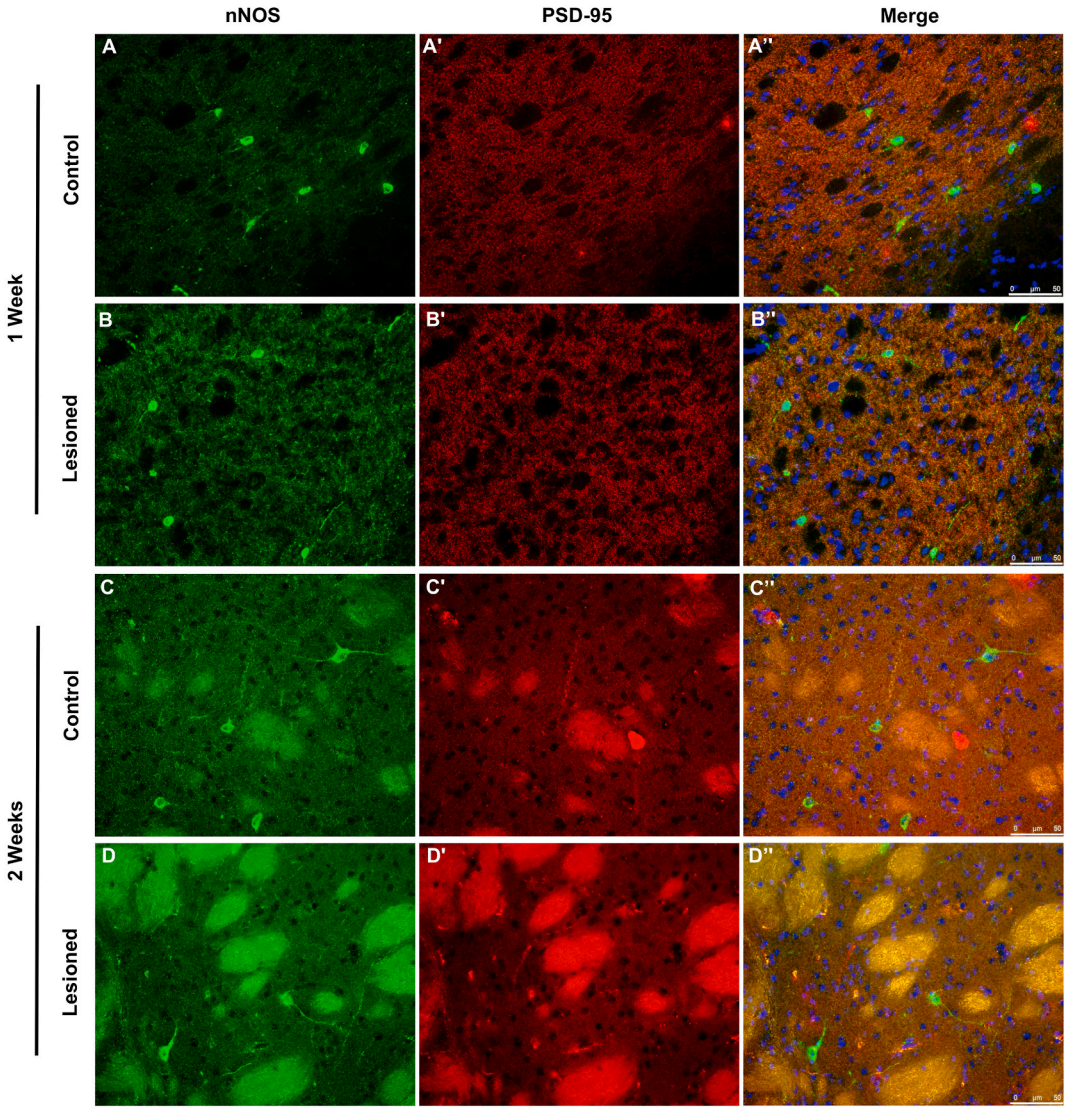

Fig. 6. Immunoreactivity of nNOS and PSD-95 in the striatum of 6-OHDA animals. Putamen region with 1 week (A, B) and 2 weeks (C, D) of survival time post-lesion. (A–D) nNOS (green) immunoreactivity. (A′-D′) PSD-95 (red) immunoreactivity. (A″-D″) Merge images revealed the overlapping of nNOS and PSD-95 in yellow, indicating a strong spatial correlation between these proteins on both sides, control and lesion, especially in the neuropile region. n = 3 animals/group. 40x. Scale bar: 50 μm.

astrocytes reactivity. Also, the authors showed that pro-inflammatory markers such as TNFα and iNOS are temporarily correlated to microglia activation [46]. However, we cannot exclude that late astrocytic activation is related to the increase in NO metabolites found in the serum after 4 weeks of injury (Fig. 5). Lan and colleagues (2022) reported that NO release and VEGFA by astrocytes treated with oligomeric α-synuclein could be related to blood brain barrier disruption in PD mice and patients (2022). Interestingly we have recently shown a biphasic increase in GFAP in the neuromuscular layer at 1 w and 4 w after 6-OHDA striatal lesion [19]. Therefore, it is plausible that iNOS in GFAP-positive astrocytes could be related to systemic effects that follows central lesion. Further studies are needed to understand this issue.

Taken together, these results demonstrate that mice injected with 6-OHDA were effectively lesioned, since major behavioral and glial responses are present during this period. Thus, the investigation of the time-course of possible synaptic alterations resulting from dopaminergic loss becomes possible and interesting, in this degeneration window.

In the central nervous system (CNS), the balance between excitatory (E) and inhibitory (I) activity is essential for proper brain function [52]. Therefore, an E-I imbalance may lead to pathological conditions, and it has been implicated in neurodegenerative diseases [53,54]. In Parkinson's disease, the E-I imbalance in the striatum appears to be due to alterations in several modulatory systems [30,55,56].

The ultrastructure of the synapses in the striatum was evaluated in 6-OHDA mice after a two-week post-lesion survival since at this

time the motor deficits were more pronounced. Interestingly, our data pointed to a decrease in total synaptic density but an increase in proportion of asymmetric (excitatory) synapses. This apparent paradox appears to be counterbalanced by the tendency for symmetrical (inhibitory) synapses to decrease on the injured side compared to the paired control (Fig. 3). This loss of synaptic structures seems to be a natural consequence of the injection of the neurotoxin 6-OHDA and the increase in excitatory synapses reveals an E-I imbalance in our animals. Therefore, we decided to investigate the glutamatergic excitatory pathway, especially NMDAR which has been implicated not only in worsening motor symptoms of PD patients and animal models but also to adverse effects of long-term dopaminergic treatment in PD [12,13]. The NMDAR function is completely regulated by the combination of different subunits forming the channel. Depending on this composition, it is related to survival or cellular death signaling pathways [57] or for synaptic strengthening or weakening [58]. It was previously reported, in the rat 6-OHDA model, striatal changes in NMDARs subunit expression and phosphorylation [12]. So, we decided to investigate the content of the main NMDA subunits in the striatum over the time. Our results showed a slight decrease in the constitutive GluN1 subunit and a transient increase in GluN2A and decrease in GluN2B, one-week post-lesion. At two weeks, an increase in GluN1 content was observed compared to the non-lesioned side. The GluN2B subunit was decreased again after four weeks of survival (Fig. 4). These data showed a rapid and dynamic regulation in the NMDAR structure and function over the course of the disease. In the postsynaptic density NMDAR is physically associated with scaffolding protein PSD-95, which organizes the molecular architecture of postsynaptic sites and impacts synaptic plasticity [59]. Here we demonstrated that PSD-95 content was also increased in the lesioned striatum of the 6-OHDA animals at all times of survival (Fig. 4). This is in accordance with previous studies that showed a change in synaptic GluN2A/GluN2B ratio as well as in GluN2D subunit associated with PSD-95 in the striatum of levodopa-treated dyskinetic rats and monkeys as well as in post-mortem tissue from dyskinetic PD patients [60–62]. In MPTP-treated marmosets, no change in GluN1 subunit was detected but both GluN2B and PSD-95 have increased [63]. On the other hand, changes in striatal NMDA receptor subunits associated with the development of dyskinesia was demonstrated in the MPTP-lesioned primate [64]. Also, an impairment in NMDAR and AMPAR-mediated signaling and currents was observed in the hippocampal neurons after Parkin mutation/loss-of-function suggesting that disrupts in glutamatergic neurotransmission also contribute to PD in this model [65].

It has been shown that PSD-95 is physically linked to the neuronal isoform of the nitric oxide synthase (nNOS), leading to an increase in nitric oxide synthesis [66].

The nNOS was transiently increased in the striatum one week after surgery (Fig. 5A and B). Interestingly, an increase in nitrates and nitrites was detected in the striatum in the same period. Therefore, we can suppose that this increase reflects greater NO production. On the other hand, in the serum, NOx increased only after four weeks (Fig. 5D), suggesting that striatal lesion may lead to systemic changes. Indeed, we recently demonstrated that 6-OHDA mice exhibit enteric inflammation and gastrointestinal dysfunction up to 4 weeks after striatal injury [19]. This is an interesting issue that should be investigated in more detail in the future.

The immunofluorescence of putamen showed a colocalization between nNOS and PSD-95 even at two weeks survival (Fig. 6). The increase in NOx and the cellular distribution of nNOS and PSD-95 demonstrated in this work are consistent with a strong interaction between NMDAR/PSD-95 and nitric oxide signaling previously demonstrated in synaptosomal membrane fractions isolated from cerebral cortex after acute effect of a histamine H1 receptor antagonist [31]. Indeed, it was demonstrated that inhibition of PSD-95/nNOS pathway reduces MPP(+)-induced neuronal injury and apoptotic cell death in cortical neurons in vitro [34]. As it was previously demonstrated, under physiological conditions, NO could mediate a feedback inhibition of NMDAR [67]. Therefore, we believe that the rapid and transient increase in NO in one week may be occurring to promote negative feedback on NMDAR function, which is increased by the prevalence of GluN2a subunit, which is known to promote an enhanced and sustained synaptic current. However, since, two-weeks after lesion, NO returns to control levels and NMDAR/PSD-95 contents increase, this sustained hyperactivation of NMDAR contributes to the increase in motor impairment.

Providing a ground for translational studies, we demonstrated, for the first time, the time-course of changes in NMDA receptor composition that could be explored as a pharmacological tool in different stages of Parkinson's disease.

Funding

This work was supported by grants from Conselho Nacional de Desenvolvimento Científico e Tecnológico (CNPq; Finance Code 304414/2018-2), Fundação Carlos Chagas Filho de Amparo à Pesquisa do Estado do Rio de Janeiro (FAPERJ; Finance Codes (E−26/200715/2017, E−26/202925/2019) e PROPPi-UFF. This study was also financed in part by the Coordenação de Aperfeiçoamento de Pessoal de Nível Superior (CAPES; Finance Code 001). Michele Barboza de Carvalho and Bruna Teixeira-Silva were recipients of a CAPES fellowship.

Data availability statement

Data will be made available on request.

CRediT authorship contribution statement

Michele Barboza de Carvalho: Writing – original draft, Methodology, Investigation, Formal analysis, Data curation. **Bruna Teixeira-Silva:** Writing – original draft, Methodology, Investigation, Formal analysis, Data curation. **Suelen Adriani Marques:** Writing – review & editing, Methodology, Formal analysis. **Andrea Alice Silva:** Writing – review & editing, Methodology, Formal analysis, Data curation. **Marcelo Cossenza:** Writing – review & editing, Formal analysis, Data curation. **Adriana da Cunha Faria-**

Melibeu: Writing – review & editing, Formal analysis. **Claudio Alberto Serfaty:** Writing – review & editing, Resources. **Paula Campello-Costa:** Writing – review & editing, Supervision, Resources, Project administration, Investigation, Funding acquisition, Formal analysis, Conceptualization.

Declaration of competing interest

The authors declare that they have no known competing financial interests or personal relationships that could have appeared to influence the work reported in this paper.

Acknowledgments

We thank Dr. Fabio Otero Ascoli for help with anesthetic procedures, Mrs Maria da Conceição Paiva Silva and Maria Leite Eduardo Pontes for technical support; Mr. Bernardino Matheus-dos-Santos (In memoriam) and Arnaldo Geraldo for animal care. We are grateful for the use of the multiuser Electron Microscopy Platform of the Institute of Biology of Fluminense Federal University (PMEIB-UFF).

Appendix A. Supplementary data

Supplementary data to this article can be found online at https://doi.org/10.1016/j.heliyon.2024.e34120.

References

[1] C. Raza, R. Anjum, N.U.A. Shakeel, Parkinson's disease: mechanisms, translational models and management strategies, Life Sci. 1 (226) (2019) 77–90, https://doi.org/10.1016/j.lfs.2019.03.057.
[2] R. Balestrino, A.H.V. Schapira, Parkinson disease, Eur. J. Neurol. 27 (1) (2020) 27–42, https://doi.org/10.1111/ene.14108.
[3] A.H.V. Schapira, K.R. Chaudhuri, P. Jenner, Non-motor features of Parkinson disease, Nat. Rev. Neurosci. 18 (7) (2017) 435–450, https://doi.org/10.1038/nrn.2017.62.
[4] J. Benkert, S. Hess, S. Roy, D. Beccano-Kelly, N. Wiederspohn, J. Duda, C. Simons, K. Patil, A. Gaifullina, N. Mannal, E. Dragicevic, D. Spaich, S. Müller, J. Nemeth, H. Hollmann, N. Deuter, Y. Mousba, C. Kubisch, C. Poetschke, J. Striessnig, O. Pongs, T. Schneider, R. Wade-Martins, S. Patel, R. Parlato, T. Frank, P. Kloppenburg, B. Liss, Cav2.3 channels contribute to dopaminergic neuron loss in a model of Parkinson's disease, Nat. Commun. 8 10 (1) (2019) 5094, https://doi.org/10.1038/s41467-019-12834-x.
[5] E. Guatteo, N. Berretta, V. Monda, A. Ledonne, N.B. Mercuri, Pathophysiological features of nigral dopaminergic neurons in animal models of Parkinson's disease, Int. J. Mol. Sci. 23 (9) (2022) 4508, https://doi.org/10.3390/ijms23094508.
[6] D.O. Borroto-Escuela, A.O. Tarakanov, I. Brito, K. Fuxe, Glutamate heteroreceptor complexes in the brain, Pharmacol. Rep. 70 (5) (2018) 936–950, https://doi.org/10.1016/j.pharep.2018.04.002.
[7] X. Fan, W.Y. Jin, Y.T. Wang, The NMDA receptor complex: a multifunctional machine at the glutamatergic synapse, Front. Cell. Neurosci. 10 (8) (2014) 160, https://doi.org/10.3389/fncel.2014.00160.
[8] C. Fiorentini, F. Gardoni, P. Spano, M. Di Luca, C. Missale, Regulation of dopamine D1 receptor trafficking and desensitization by oligomerization with glutamate N-methyl-D-aspartate receptors, J. Biol. Chem. 278 (22) (2003) 20196–20202, https://doi.org/10.1074/jbc.M213140200.
[9] K.B. Hansen, F. Yi, R.E. Perszyk, F.S. Menniti, S.F. Traynelis, NMDA receptors in the central nervous system, Methods Mol. Biol. 1677 (2017) 1–80, https://doi.org/10.1007/978-1-4939-7321-7_1.
[10] K.B. Hansen, F. Yi, R.E. Perszyk, H. Furukawa, L.P. Wollmuth, A.J. Gibb, S.F. Traynelis, Structure, function, and allosteric modulation of NMDA receptors, J. Gen. Physiol. 150 (8) (2018) 1081–1105, https://doi.org/10.1085/jgp.201812032.
[11] L. Franchini, J. Stanic, L. Ponzoni, M. Mellone, N. Carrano, S. Musardo, E. Zianni, G. Olivero, E. Marcello, A. Pittaluga, M. Sala, C. Bellone, C. Racca, M. Di Luca, F. Gardoni, Linking NMDA receptor synaptic retention to synaptic plasticity and cognition, iScience 19 (2019) 927–939, https://doi.org/10.1016/j.isci.2019.08.036.
[12] A.W. Dunah, Y. Wang, R.P. Yasuda, K. Kameyama, R.L. Huganir, B.B. Wolfe, D.G. Standaert, Alterations in subunit expression, composition, and phosphorylation of striatal N-methyl-D-aspartate glutamate receptors in a rat 6-hydroxydopamine model of Parkinson's disease, Mol. Pharmacol. 57 (2) (2000) 342–352, https://doi.org/10.3233/JPD-181474, 1064864.
[13] K.D. Küppenbender, D.G. Standaert, T.J. Feuerstein, Jr J.B. Penney, A.B. Young, G.B. Landwehrmeyer, Expression of NMDA receptor subunit mRNAs in neurochemically identified projection and interneurons in the human striatum, Comp Neurol 419 (4) (2000) 407–421, https://doi.org/10.1002/(sici)1096-9861(20000417)419:4<407::aid-cne1>3.0.co;2-i.
[14] M.L. Blanke, A.M.J. VanDongen, Activation mechanisms of the NMDA receptor, in: A.M. Van Dongen (Ed.), Biology of the NMDA Receptor, CRC Press/Taylor & Francis, Boca Raton (FL), 2009 (Chapter 13).
[15] I. Ahmed, S.K. Bose, N. Pavese, A. Ramlackhansingh, F. Turkheimer, G. Hotton, A. Hammers, D.J. Brooks, Glutamate NMDA receptor dysregulation in Parkinson's disease with dyskinesias, Brain 134 (Pt 4) (2011) 979–986, https://doi.org/10.1093/brain/awr028.
[16] P. Paoletti, C. Bellone, Q. Zhou, NMDA receptor subunit diversity: impact on receptor properties, synaptic plasticity and disease, Nat. Rev. Neurosci. 14 (6) (2013) 383–400, https://doi.org/10.1038/nrn3504.
[17] H. Xu, X. Liu, J. Xia, T. Yu, Y. Qu, H. Jiang, J. Xie, Activation of NMDA receptors mediated iron accumulation via modulating iron transporters in Parkinson's disease, Faseb. J. 13 (2018) fj201800060RR, https://doi.org/10.1096/fj.201800060RR.
[18] C. Maccallini, R. Amoroso, Targeting neuronal nitric oxide synthase as a valuable strategy for the therapy of neurological disorders, Review Neural Regen Res (11) (2016) 1731–1734, https://doi.org/10.4103/1673-5374.194707.
[19] B.B.M. Thomasi, L. Valdetaro, M.C.G. Ricciardi, L. Hayashide, A.C.M.N. Fernandes, A. Mussauer, M.L. da Silva, A. da Cunha Faria-Melibeu, M.G.L. Ribeiro, J. de Mattos Coelho-Aguiar, P. Campello-Costa, V. Moura-Neto, A.L. Tavares-Gomes, Enteric glial cell reactivity in colonic layers and mucosal modulation in a mouse model of Parkinson's disease induced by 6-hydroxydopamine, Brain Res. Bull. 187 (2022) 111–121, https://doi.org/10.1016/j.brainresbull.2022.06.013.
[20] J.M. Klug, A.B. Norman, Long-term sensitization of apomorphine-induced rotation behavior in rats with dopamine deafferentation or excitotoxin lesions of the striatum, Pharmacol. Biochem. Behav. 46 (2) (1993) 397–403, https://doi.org/10.1016/0091-3057(93)90370-9, 1993.
[21] M.M. Bradford, A rapid and sensitive method for the quantitation of microgram quantities of protein utilizing the principle of protein-dye binding, Anal. Biochem. 72 (1976) 248–274.

[22] C.M. Carvalho, J.C. Silverio, A.A. da Silva, I.R. Pereira, J.M.C. Coelho, C.C. Britto, O.C. Moreira, R.S. Marchevsky, S.S. Xavier, R.T. Gazzinelli, M.G. Bonecini-Almeida, J. Lannes-Vieira, Inducible nitric oxide synthase in heart tissue and nitric oxide in serum of Trypanosoma cruzi-infected rhesus monkeys: association with heart injury, PLoS Neglected Trop. Dis. 6 (2012) e1644, https://doi.org/10.1371/journal.pntd.0001644.

[23] K.M. Miranda, M.G. Espey, D.A. Wink, A rapid, simple spectrophotometric method for simultaneous detection of nitrate and nitrite, Nitric Oxide 1 (2001) 62–71, https://doi.org/10.1006/niox.2000.0319.

[24] L. Forny-Germano, N.M. Lyra e Silva, A.F. Batista, J. Brito-Moreira, M. Gralle, S.E. Boehnke, B.C. Coe, A. Lablans, S.A. Marques, A.M. Martinez, W.L. Klein, J. C. Houzel, S.T. Ferreira, D.P. Munoz, F.G. De Felice, Alzheimer's disease-like pathology induced by amyloid-β oligomers in nonhuman primates, J. Neurosci. 34 (41) (2014) 13629–13643, https://doi.org/10.1523/jneurosci.1353-14.2014.

[25] D. Alvarez-Fischer, C. Henze, C. Strenzke, J. Westrich, B. Ferger, G.U. Höglinger, W.H. Oertel, A. Hartmann, Characterization of the striatal 6-OHDA model of Parkinson's disease in wild type and alpha-synuclein-deleted mice, Exp. Neurol. 210 (1) (2007) 182–193, https://doi.org/10.1016/j.expneurol.2007.10.012.

[26] V. Bagga, S.B. Dunnett, R.A. Fricker, The 6-OHDA mouse model of Parkinson's disease - terminal striatal lesions provide a superior measure of neuronal loss and replacement than median forebrain bundle lesions, Behav. Brain Res. 15 (288) (2015) 107–117, https://doi.org/10.1016/j.bbr.2015.03.058.

[27] L. Lovino, M.E. Tremblay, L. Civiero, Glutamate-induced excitotoxicity in Parkinson's disease: the role of glial cells, J. Pharmacol. Sci. 144 (3) (2020) 151–164, https://doi.org/10.1016/j.jphs.2020.07.011.

[28] S. Smajić, C.A. Prada-Medina, Z. Landoulsi, J. Ghelfi, S. Delcambre, C. Dietrich, J. Jarazo, J. Henck, S. Balachandran, S. Pachchek, C.M. Morris, P. Antony, B. Timmermann, S. Sauer, S.L. Pereira, J.C. Schwamborn, P. May, A. Grünewald, M. Spielmann, Single-cell sequencing of human midbrain reveals glial activation and a Parkinson-specific neuronal state, Brain 145 (3) (2022) 964–978, https://doi.org/10.1093/brain/awab446.

[29] Y. Iwasaki, K. Ikeda, T. Shiojima, M. Kinoshita, Increased plasma concentrations of aspartate, glutamate and glycine in Parkinson's disease, Neurosci. Lett. 145 (2) (1992) 175–177, https://doi.org/10.1016/0304-3940(92)90015-y.

[30] R.L. O'Gorman Tuura, C.R. Baumann, H. Baumann-Vogel, Beyond dopamine: GABA, glutamate, and the axial symptoms of Parkinson disease, Front. Neurol. 26 (9) (2018) 806, https://doi.org/10.3389/fneur.2018.00806.

[31] S. Lores-Arnaiz, A.G. Karadayian, A. Gutnisky, J. Miranda, Arnaiz G. Rodríguez de Lores, Changes in synaptic proteins of the complex PSD-95/NMDA receptor/nNOS and mitochondrial dysfunction after levocabastine treatment, Neurochem. Int. 148 (2021) 105100, https://doi.org/10.1016/j.neuint.2021.105100.

[32] K.S. Christopherson, B.J. Hillier, W.A. Lim, D.S. Bredt, PSD-95 assembles a ternary complex with the N-methyl-D-aspartic acid receptor and a bivalent neuronal NO synthase PDZ domain, J. Biol. Chem. 274 (39) (1999) 27467–27473, https://doi.org/10.1074/jbc.274.39.27467.

[33] F.J. Jiménez-Jiménez, H. Alonso-Navarro, M.T. Herrero, E. García-Martín, J.A.G. Agúndez, An update on the role of nitric oxide in the neurodegenerative processes of Parkinson's disease, Curr. Med. Chem. (24) (2016) 2666–2679, https://doi.org/10.2174/0929867323666160812151356.

[34] W. Hu, L.S. Guan, X.B. Dang, P.Y. Ren, Y.L. Zhang, Small-molecule inhibitors at the PSD-95/nNOS interface attenuate MPP+-induced neuronal injury through Sirt3 mediated inhibition of mitochondrial dysfunction, Neurochem. Int. 79 (2014) 57–64, https://doi.org/10.1016/j.neuint.2014.10.005.

[35] E.R. Dorsey, T. Sherer, M.S. Okun, B.R. Bloem, The emerging evidence of the Parkinson pandemic, J. Parkinsons Dis. 8 (s1) (2018) S3–S8, https://doi.org/10.3233/JPD-181474.

[36] E. Bezard, C. Imbert, C.E. Gross, Experimental models of Parkinson's disease: from the static to the dynamic, Rev. Neurosci. 9 (1998) 71–90, https://doi.org/10.1515/revneuro.1998.9.2.71.

[37] E. Bezard, S. Przedborski, A tale on animal models of Parkinson's disease, Mov. Disord. 26 (2011) 6 993–1002, https://doi.org/10.1002/mds.23696.

[38] K. Tieu, A guide to neurotoxic animal models of Parkinson's disease, Spring Harb Perspect Med 1 (1) (2011) a009316, https://doi.org/10.1101/cshperspect.a009316.

[39] F. Blandini, G. Levandis, E. Bazzini, G. Nappi, M.T. Armentero, Time-course of nigrostriatal damage, basal ganglia metabolic changes and behavioural alterations following intrastriatal injection of 6-hydroxydopamine in the rat: new clues from an old model, Eur. J. Neurosci. 25 (2) (2007) 397–405, https://doi.org/10.1111/j.1460-9568.2006.05285.x.

[40] F. Blandini, M.T. Armentero, Animal models of Parkinson's disease, FEBS J. 279 (7) (2012) 1156–1166, https://doi.org/10.1111/j.1742-4658.2012.08491.x.

[41] A. Tamás, A. Lubics, L. Szalontay, I. Lengvári, D. Reglődi, Age and gender differences in behavioral and morphological outcome after 6-hydroxydopamine-induced lesion of the substantia nigra in rats, Behav. Brain Res. 158 (2) (2005) 221–229, https://doi.org/10.1016/j.bbr.2004.09.002.

[42] G.E. Gillies, I.S. Pienaar, S.V.Z. Qamhawi, Sex differences in Parkinson's disease, Front. Neuroendocrinol. 35 (3) (2014) 370–384, https://doi.org/10.1016/j.yfrne.2014.02.002.

[43] F. Blandini, M.T. Armentero, E. Martignoni, The 6-hydroxydopamine model: news from the past, Parkinsonism Relat. Disorders 14 (2) (2008) S124–S129.

[44] F. Campanelli, G. Natale, G. Marino, V. Ghiglieri, P. Calabresi, Striatal glutamatergic hyperactivity in Parkinson's disease, Neurobiol. Dis. 168 (2022) 105697, https://doi.org/10.1016/j.nbd.2022.105697.

[45] P. Gonzalez-Latapi, S.S. Bhowmick, G. Saranza, S.H. Fox, Non-dopaminergic treatments for motor control in Parkinson's disease: an update, CNS Drugs 34 (10) (2020) 1025–1044, https://doi.org/10.1007/s40263-020-00754-0.

[46] S.J.P. Haas, X. Zhou, V. Machado, A. Wree, K. Krieglstein, B. Spittau, Expression of TGFβ1 and inflammatory markers in the 6-hydroxydopamine mouse model of Parkinson's disease, Front. Mol. Neurosci. 9 (2016) 7, https://doi.org/10.3389/fnmol.2016.00007.

[47] H.D.E. Booth, W.D. Hirst, R. Wade-Martins, The role of astrocyte dysfunction in Parkinson's disease pathogenesis, Trends Neurosci. 40 (6) (2017) 358–370, https://doi.org/10.1016/j.tins.2017.04.001.

[48] T.I. Kam, J.T. Hinkle, T.M. Dawson, V.L. Dawson, Microglia and astrocyte dysfunction in Parkinson's disease, Neurobiol. Dis. 144 (2020) 105028, https://doi.org/10.1016/j.nbd.2020.105028.

[49] K. Badanjak, S. Fixemer, S. Smajić, A. Skupin, A. Grünewald, The contribution of microglia to neuroinflammation in Parkinson's disease, Int. J. Mol. Sci. 22 (9) (2021) 4676, https://doi.org/10.3390/ijms22094676.

[50] B. Mendes-Pinheiro, C. Soares-Cunha, A. Marote, E. Loureiro-Campos, J. Campos, S. Barata-Antunes, D. Monteiro-Fernandes, D. Santos, S. Duarte-Silva, L. Pinto, A.J. Salgado, Unilateral intrastriatal 6-hydroxydopamine lesion in mice: a closer look into non-motor phenotype and glial response, Int. J. Mol. Sci. 22 (21) (2021) 11530, https://doi.org/10.3390/ijms222111530.

[51] K. Kuter, L. Olech, U. Głowacka, Prolonged dysfunction of astrocytes and activation of microglia accelerate degeneration of dopaminergic neurons in the rat substantia nigra and block compensation of early motor dysfunction induced by 6-OHDA, Mol. Neurobiol. (4) (2018) 3049–3066, https://doi.org/10.1007/s12035-017-0529-z.

[52] S. Zhou, Y. Yu, E.-I. Synaptic, Balance underlies efficient neural coding, Front. Neurosci. 12 (2018) 46, https://doi.org/10.3389/fnins.2018.00046.

[53] S. Ghatak, M. Talantova, S.R. McKercher, S.A. Lipton, Novel therapeutic approach for excitatory/inhibitory imbalance in neurodevelopmental and neurodegenerative diseases, Annu. Rev. Pharmacol. Toxicol. 61 (2021) 701–721, https://doi.org/10.1146/annurev-pharmtox-032320-015420.

[54] V.E. Varela, G. Etter, S. Williams, Excitatory-inhibitory imbalance in Alzheimer's disease and therapeutic significance, Neurobiol. Dis. 127 (2019) 605–615, https://doi.org/10.1016/j.nbd.2019.04.010.

[55] A. Pinna, M. Serra, M. Morelli, N. Simola, Role of adenosine A2A receptors in motor control: relevance to Parkinson's disease and dyskinesia, J. Neural. Transm. 125 (8) (2018) 1273–1286, https://doi.org/10.1007/s00702-018-1848-6.

[56] M. Padilla-Orozco, M. Duhne, A. Fuentes-Serrano, A. Ortega, E. Galarraga, J. Bargas, E. Lara-González, Synaptic determinants of cholinergic interneurons hyperactivity during parkinsonism, Front. Synaptic Neurosci. 6 (14) (2022) 945816, https://doi.org/10.3389/fnsyn.2022.945816.

[57] B. Lujan, X. Liu, Q. Wan, Differential roles of GluN2A- and GluN2B-containing NMDA receptors in neuronal survival and death, Int J Physiol Pathophysiol Pharmacol 4 (4) (2012) 211–218.

[58] O.A. Shipton, O. Paulsen, GluN2A and GluN2B subunit-containing NMDA receptors in hippocampal plasticity, Philos. Trans. R. Soc. Lond. B Biol. Sci. 369 (1633) (2014) 20130163, https://doi.org/10.1098/rstb.2013.0163.

[59] X. Chen, J.M. Levy, A. Hou, C. Winters, R. Azzam, A.A. Sousa, R.D. Leapman, R.A. Nicoll, T.S. Reese, PSD-95 family MAGUKs are essential for anchoring AMPA and NMDA receptor complexes at the postsynaptic density, Proc. Natl. Acad. Sci. U.S.A. 15 112 (50) (2015) E6983–E6992, https://doi.org/10.1073/pnas.1517045112.

[60] M. Mellone, J. Stanic, L.F. Hernandez, E. Iglesias, E. Zianni, A. Longhi, A. Prigent, B. Picconi, P. Calabresi, E.C. Hirsch, J.A. Obeso, M. Di Luca, F. Gardoni, NMDA receptor GluN2A/GluN2B subunit ratio as synaptic trait of levodopa-induced dyskinesias: from experimental models to patients, Front. Cell. Neurosci. 6 (9) (2015) 245, https://doi.org/10.3389/fncel.2015.00245.

[61] M. Mellone, E. Zianni, J. Stanic, F. Campanelli, G. Marino, V. Ghiglieri, A. Longhi, M.L. Thiolat, Q. Li, P. Calabresi, E. Bezard, B. Picconi, M. Di Luca, F. Gardoni, NMDA receptor GluN2D subunit participates to levodopa-induced dyskinesia pathophysiology, Neurobiol. Dis. 121 (2019) 338–349, https://doi.org/10.1016/j.nbd.2018.09.021.

[62] G. Sitzia, I. Mantas, X. Zhang, P. Svenningsson, K. Chergui, NMDA receptors are altered in the substantia nigra pars reticulata and their blockade ameliorates motor deficits in experimental parkinsonism, Neuropharmacology 174 (2020) 108136, https://doi.org/10.1016/j.neuropharm.2020.108136.

[63] M.J. Hurley, M.J. Jackson, L.A. Smith, S. Rose, P. Jenner, Immunoautoradiographic analysis of NMDA receptor subunits and associated postsynaptic density proteins in the brain of dyskinetic MPTP-treated common marmosets, Eur. J. Neurosci. 12 (2005) 3240–3250, https://doi.org/10.1111/j.1460-9568.2005.04169.x.

[64] P.J. Hallett, A.W. Dunah, P. Ravenscroft, S. Zhou, E. Bezard, A.R. Crossman, J.M. Brotchie, D.G. Standaert, Alterations of striatal NMDA receptor subunits associated with the development of dyskinesia in the MPTP-lesioned primate model of Parkinson's disease, Neuropharmacology 48 (4) (2005) 503–516, https://doi.org/10.1016/j.neuropharm.2004.11.008.

[65] M. Zhu, G.P. Cortese, C.L. Waites, Parkinson's disease-linked Parkin mutations impair glutamatergic signaling in hippocampal neurons, BMC Biol. 16 (1) (2018) 100, https://doi.org/10.1186/s12915-018-0567-7.

[66] Y. Gu, D. Zhu, nNOS-mediated protein-protein interactions: promising targets for treating neurological and neuropsychiatric disorders, J Biomed Res 35 (1) (2020) 1–10, https://doi.org/10.7555/JBR.34.20200108.

[67] S.R. Chen, X.G. Jin, H.L. Pan, Endogenous nitric oxide inhibits spinal NMDA receptor activity and pain hypersensitivity induced by nerve injury, Neuropharmacology 125 (2017) 156–165, https://doi.org/10.1016/j.neuropharm.2017.07.023.